in δ value, discussions in the text are mainly based on the latter values. Concentration of the sample was *ca.* 15% (wt/v) except for $[Et_2AlOLi][AlEt_3]$ (~2%) due to low solubility. The spectra showed no signals at δ 4–6 ppm due to oxidized species which might be produced by ill handling of the organoaluminums under argon atmosphere by syringes.

The spin-tickling experiment was performed using a Varian T-60 spectrometer with weak-field double irradiation in the frequency sweep mode. A Japan Optics Laboratory Co. Ltd. JNM-4H-100 spectrometer was used for the measurements at 100 MHz.

Registry No. $[Et_2AlOLi][AlEt_3]$, 15407-37-1; $[Et_2AlONa][AlEt_3]$, 18347-70-1; $[Et_2AlOK][AlEt_3]$, 29467-77-4; $[Et_2AlOCs][AlEt_3]$, 38118-15-9; $[Et_2AlNPhLi][AlEt_3]$, 25136-39-4; $[Et_2AlSNa][AlEt_3]$, 38118-17-1; $[(i\text{-Bu})_2AlOLi][Al(i\text{-Bu})_3]$, 38194-35-3; $[(i\text{-Bu})_2AlONa][Al(i\text{-Bu})_3]$, 38118-18-2; $[(i\text{-Bu})_2AlOK][Al(i\text{-Bu})_3]$, 38118-19-3; $[(i\text{-Bu})_2AlOCs][Al(i\text{-Bu})_3]$, 38118-20-6; $[(i\text{-Bu})_2AlNPhLi][Al(i\text{-Bu})_3]$, 38194-36-4; $[Et_2AlONa][AlMe_3]$, 38118-21-7; $[Et_2AlOLi][AlMe_3][THF]$, 38118-22-8; $[Me_2AlOLi][AlMe_3][THF]$, 38118-23-9; $[Et_2AlOLi][AlEt_3][THF]$, 38118-24-0; $[Et_2AlONa][AlEt_3][THF]$, 38118-25-1; $[(i\text{-Bu})_2AlOK][Al(i\text{-Bu})_3][THF]$, 38118-26-2.

Acknowledgment. We wish to thank Mr. Masatoshi Mikumo for his experiments on the sulfur-containing compound, Mr. Shintaro Tachibana for the high-vacuum synthesis of $[Et_2AlOLi][AlEt_3]$, and Mr. Muneo Fukui for the synthesis of deuterated toluene. We also wish to express our appreciation to Dr. E. J. Vandenberg of Hercules Powder Co., for a gift of toluene-d_8. We are grateful to Mr. H. Naoki, Mr. M. Doi, and Miss Y. Kawashima for their running of nmr spectra.

Contribution No. 4240 from the Arthur Amos Noyes Laboratory of Chemical Physics,
California Institute of Technology, Pasadena, California 91109

Spectroscopic and Magnetic Properties of Heptacyanomolybdate(III). Evidence for Pentagonal-Bipyramidal and Monocapped Trigonal-Prismatic Structures

GEORGE R. ROSSMAN, F.-D. TSAY, and HARRY B. GRAY*

Received August 10, 1972

Several salts containing the $Mo(CN)_7^{4-}$ ion have been studied by a variety of spectroscopic and magnetic techniques. Infrared and Raman spectral data together with magnetic susceptibility measurements suggest a pentagonal-bipyramidal (D_{5h}) structure ($^2E_1''(e_1'')^3$ ground state) for $Mo(CN)_7^{4-}$ in aqueous solutions of $K_4Mo(CN)_7 \cdot 2H_2O$. Anhydrous $K_4Mo(CN)_7$ and solid $Cs_4Mo(CN)_7 \cdot xH_2O$ also appear to contain pentagonal-bipyramidal anions. Solid $K_4Mo(CN)_7 \cdot 2H_2O$, however, exhibits infrared and Raman spectra that differ from the aqueous solution results. The esr spectrum of the dihydrate, which can be observed only below 150°K, gives $g_\parallel = 2.103$ and $g_\perp = 1.973$. The g values and a $\mu_{\text{eff}} = 1.73$ BM are consistent with a $^2A_1(a_2)^2(a_1)^1$ ground state of a monocapped trigonal-prismatic (C_{2v}) coordination geometry. Electronic spectral bands at 16,100, 20,900, and 22,500 cm^{-1} in crystalline $K_4Mo(CN)_7 \cdot 2H_2O$ are assigned respectively to the d–d transitions $^2A_1 \rightarrow {}^2A_2$, $^2A_1 \rightarrow {}^2B_2$, and $^2A_1 \rightarrow {}^2B_1$. The lowest spin-allowed d–d transition in D_{5h} $Mo(CN)_7^{4-}$ occurs at 24,900 cm^{-1}.

Introduction

The complex $K_4Mo(CN)_7 \cdot 2H_2O$ was reported by Young[1] in 1932 but to date has not been well characterized by physical methods. The compound is of considerable interest in view of the apparent seven-coordinate nature of the complex anion, $Mo(CN)_7^{4-}$, but it should be recognized that formulation as a higher coordinate species such as $Mo(CN)_7H_2O^{4-}$ is also possible.

In our laboratory we have been engaged in an investigation of the physical and chemical properties of various compounds containing the $Mo(CN)_7^{4-}$ ion. Although our attempts to establish the structure of $Mo(CN)_7^{4-}$ in several solid compounds by single-crystal X-ray methods have not yet been successful, we have been able to characterize thoroughly the complex anion by spectroscopic and magnetic measurements on both solid and aqueous solution samples. In the present paper we report magnetic susceptibility results and esr, infrared, Raman, and electronic spectral data for $K_4Mo(CN)_7 \cdot 2H_2O$ and $K_4Mo(CN)_7$. For comparison, certain preliminary results are also included for $Cs_4Mo(CN)_7 \cdot xH_2O$.

Experimental Section

Preparation of Compounds. Several batches of $K_4Mo(CN)_7 \cdot 2H_2O$ were prepared from K_3MoCl_6[2] and excess KCN by the literature method.[1] Shiny black flakes of 1–3-mm size and fine, dark olive green flakes were obtained in various batches. Recrystallization was accomplished by cooling concentrated solutions in oxygen-free water–ethanol mixtures and less conveniently by cooling saturated aqueous solutions. *Anal.* Calcd for $K_4Mo(CN)_7 \cdot 2H_2O$: K, 33.24; Mo, 20.39; C, 17.87; N, 20.84; H, 0.86. Found: K, 33.05; Mo, 20.47; C, 18.05; N, 20.39; H, 0.96.

Anhydrous $K_4Mo(CN)_7$ was prepared from the hydrate by heating it for 10–15 hr at 95° under high vacuum. It was also prepared in a finely divided form by lyopholyzing aqueous solutions of the dihydrate. *Anal.* Calcd for $K_4Mo(CN)_7$: K, 36.00; Mo, 22.08; C, 19.35; N, 22.57; H, 0.00. Found: K, 34.89; Mo, 22.33; C, 19.64; N, 22.22; H, 0.00.

Infrared spectra show that both $K_4Mo(CN)_7 \cdot 2H_2O$ and $K_4Mo(CN)_7$ decompose in air to KOH, $K_4Mo(CN)_8$, and K_2MoO_4. No evidence for what has been reported[3] to be $KMo(CN)_5$ was observed in the oxidation products. Although the solid dihydrate can be briefly exposed to dry air for purposes such as weighing without any sign of decomposition, it was generally handled in a nitrogen-purged glovebag and transferred to the appropriate nitrogen-filled containers. In a dry atmosphere, the flakes of the solid readily accumulate static electricity. The compound is soluble in water and slowly soluble in ethylene glycol but was found to be insoluble in common organic solvents. Since the solutions are extremely oxygen sensitive, all sample preparations of solutions for physical measurements were done in a high-vacuum line. The appropriate amount of degassed water was sublimed onto the solids in the sample vessel and the vessels were then closed either with stopcocks or by flame sealing under vacuum.

Physical Measurements. Absorption spectra in the region 210–2500 nm were obtained on a Cary 14 RI spectrophotometer equipped with quartz dewar for immersion of samples into liquid N_2.

---

[1] R. C. Young, *J. Amer. Chem. Soc.*, **54**, 1402 (1932).

[2] R. J. Irving and M. C. Steele, *Aust. J. Chem.*, **10**, 490 (1957).

[3] M. C. Steele, *Aust. J. Chem.*, **10**, 404 (1957).

The reported position and ϵ value of each band were obtained by visually subtracting out contributions due to overlapping bands. Infrared spectra were obtained on a Perkin-Elmer 225 spectrophotometer. Pellets and mulls of oxygen-sensitive materials were prepared in nitrogen-purged glove bags. Solution spectra were obtained from samples dissolved in the vacuum line and transferred to N_2-filled BaF_2 solution cells with a syringe in a glove bag. Low-temperature infrared spectra were obtained using a modified Beckman RIIC VLT-2 unit. Raman spectra were obtained on a Cary 81 He–Ne laser Raman in flame-sealed Pyrex solution tubes and with solids on a conical powder holder. Solids were protected from slow air oxidation with mineral oil.

Electron spin resonance spectra were obtained at both X-band (9.50 GHz) and K-band (34.83 GHz) frequencies on a Varian V-4500 spectrometer using 100-kHz field modulation. The g values were determined by comparison with the resonance position of a standard DPPH sample ($g = 2.0037$). The low-temperature measurements were carried out by immersion of the cavity in liquid nitrogen or by blowing a stream of precooled nitrogen gas through the cavity. Temperature control was achieved using a Varian V-4540 variable-temperature controller.

Magnetic susceptibility data were taken on a Princeton Applied Research FM-1 vibrating-sample magnetometer system equipped with an Andonian Associates variable-temperature dewar. System calibrations were performed with $HgCo(SCN)_4$.

Results and Discussion

Infrared and Raman Spectra. Figure 1 shows the infrared and Raman spectra in the cyano stretching region of $K_4Mo(CN)_7 \cdot 2H_2O$ in aqueous solution. The infrared spectra of an approximately 0.2 F aqueous solution and an approximately 0.12 F solution in 0.1 F KOH (which minimized photodecomposition) both consist of two bands of nearly equal intensities ($\epsilon \sim 900$) at 2080 and 2040 cm^{-1}. The aqueous solution Raman spectrum, which was obtained by adding either cyanide ion or hydroxide ion to suppress rapid photodecomposition, displays two weak Raman bands of roughly comparable intensities at 2106 and 2063 cm^{-1}. The third band at 2079 cm^{-1} is attributable to added cyanide ion and is not present in the spectrum of a hydroxide-containing solution.

The observed pattern of infrared and Raman bands in aqueous solution is best accommodated by assuming that the geometrical structure of $Mo(CN)_7{}^{4-}$ in this medium is based on a pentagonal bipyramid. In D_{5h} symmetry two fundamental cyano stretching modes, $a_2{}''$ and $e_1{}'$, are infrared allowed. As three modes, $2a_1{}'$ and $e_2{}'$, are Raman allowed, it is necessary to postulate either that two of the three Raman bands are very close in energy or that the missing Raman band is of very low intensity. We emphasize, however, that the small number of observed infrared and Raman bands and, in particular, the lack of coincidences rule against seven-coordinate structures of low symmetry. We also note that a very recent X-ray investigation on $K_4V(CN)_7 \cdot 2H_2O$ by Towns and Levenson[4] has established a pentagonal-bipyramidal structure for $V(CN)_7{}^{4-}$.

We considered the possibility that dissociation of $Mo(CN)_7{}^{4-}$ in aqueous solution to yield $Mo(CN)_6{}^{3-} + CN^-$ occurs, particularly as the band at 2080 cm^{-1} in the solution infrared spectrum is at the frequency of free cyanide ion. However, the absence of this band in the Raman spectrum of $K_4Mo(CN)_7 \cdot 2H_2O$ in 0.1 F KOH as well as ligand field spectral and solution magnetic susceptibility data (*vide infra*) show that $Mo(CN)_6{}^{3-}$ is not present. A dimeric cyano-bridged formulation can also be eliminated since bridging cyanides would be expected to absorb strongly at or above 2150 cm^{-1}.

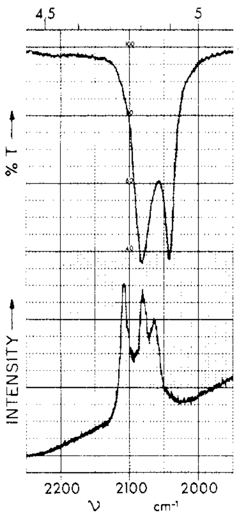

Figure 1. Infrared and Raman spectra of the cyanide stretching region of $Mo(CN)_7{}^{4-}$ in aqueous solution: upper curve, infrared spectrum of ~ 0.2 F $K_4Mo(CN)_7 \cdot 2H_2O$, ambient temperature; lower curve, Raman spectrum of $K_4Mo(CN)_7 \cdot 2H_2O$ estimated to be 0.1 F in 0.2 F aqueous KCN, ambient temperature (center band is due to uncomplexed CN^-).

The infrared spectrum of solid $K_4Mo(CN)_7 \cdot 2H_2O$ is essentially identical in mulls and KBr pellets (Figure 2). There are four regions of absorption: the water bands near 3500 and 1610 cm^{-1}, the cyanide stretches near 2070 cm^{-1}, and a broad region of absorption extending from 250 to 550 cm^{-1} corresponding to overlapping metal-carbon stretches, metal-carbon-nitrogen bends, and modes attributable to lattice water.

The water region near 3500 cm^{-1} consists of a set of moderately broad, poorly resolved, overlapping bands in both mulls and KBr pellets. At liquid nitrogen temperature, the KBr pellet spectrum develops structure. The three most prominent peaks occur at 3581, 3498, and 3428 cm^{-1}, with several partially resolved bands and shoulders between them. At room temperature, the water band at 1610 cm^{-1} has a shoulder at about 1640 cm^{-1}, whereas near 78°K, the band system sharpens markedly to reveal a peak at 1613 cm^{-1} and a broader band near 1646 cm^{-1}. In more concentrated pellets at low temperature, the shoulder near 1600 cm^{-1} also resolves into a band.

The cyanide stretching region in Nujol mulls is significantly different from the aqueous solution spectrum, consisting of a strong and somewhat broad band at about 2064 cm^{-1} and a weaker but well-resolved side band at 2111 cm^{-1}. In KBr pellets, these bands appear at 2070 and about 2114 cm^{-1}, respectively. At approximately liquid nitrogen temperature, the resolution improves to reveal a band at 2059 cm^{-1} and splitting of the 2114-cm^{-1} band into two components at 2119 and 2115 cm^{-1}. The main peak shifts to 2074 cm^{-1} and has some poorly resolved structure on the high-energy side.

A broad region of absorption with much structure is found between 250 and 500 cm^{-1}. Bands are located at 498, 436, 398, 356, 338, and 294 cm^{-1} in Nujol mulls. The bands occur at about the same positions in KBr pellets, as is shown in Figure 2. Upon partial deuteration of the dihydrate, the band at 338 cm^{-1} decreases in intensity, but no other changes are apparent in the low-energy region.

The Raman spectrum of the black solid was difficult to obtain due to absorption problems. From a coarsely ground sample of the solid, two Raman bands were obtained under conditions of high instrument gain at 2096 and 2078 cm^{-1}. With the exception of weak water bands, no other Raman

---

[4] R. L. R. Towns and R. A. Levenson, *J. Amer. Chem. Soc.*, 94, 4346 (1972).

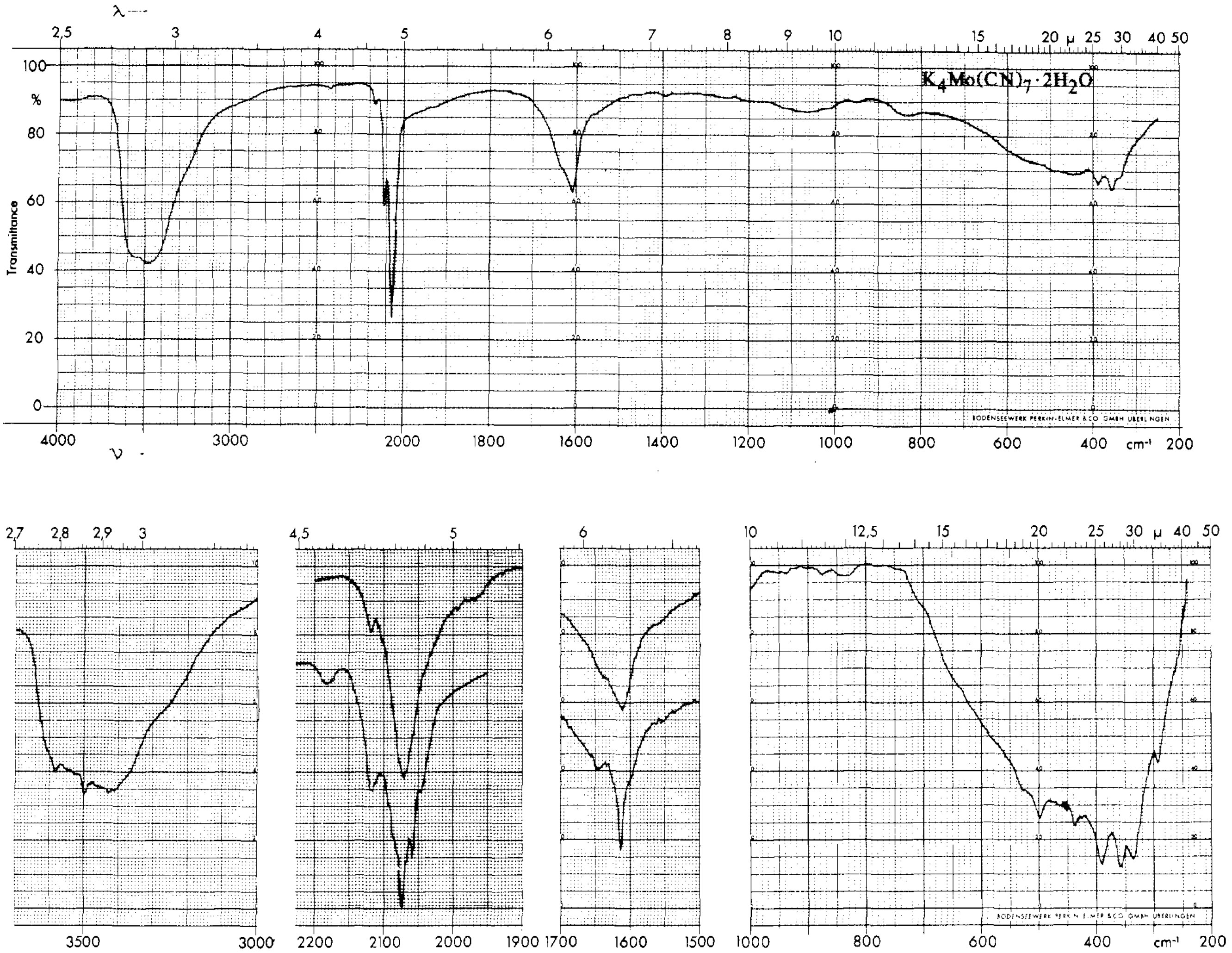

Figure 2. Infrared spectra of KBr pellets of $K_4Mo(CN)_7 \cdot 2H_2O$: top panel, 0.67 mg/400 mg of KBr, ambient temperature; bottom panels (left to right), 0.67 mg/400 mg of KBr, near 80°K; 0.67 mg/400 mg of KBr, upper curve–ambient temperature and lower curve–near 80°K; 0.67 mg/400 mg of KBr, upper curve–ambient temperature and lower curve–near 80°K; 7.6 mg/400 mg of KBr, ambient temperature.

frequencies were observed. In spite of the experimental difficulties, it is evident that the Raman results support the infrared spectral comparisons which indicate that the geometrical structures of $Mo(CN)_7{}^{4-}$ in solid $K_4Mo(CN)_7 \cdot 2H_2O$ and in aqueous solution are different. We shall defer assignment of the $Mo(CN)_7{}^{4-}$ structure in the solid potassium dihydrate salt until the esr data are considered.

The infrared spectrum of either a mull or KBr pellet of the anhydrous potassium salt, $K_4Mo(CN)_7$, in the cyano stretching region shows bands at about 2078 and 2046 cm^{-1}. These two bands are very similar in both position and shape to the two bands observed in an aqueous solution of $K_4Mo(CN)_7 \cdot 2H_2O$. The remainder of the spectrum of $K_4Mo(CN)_7$ simplifies as compared to the solid dihydrate from the loss of the water bands and the appearance of a single medium-intensity band at 358 cm^{-1} and a weaker band at 432 cm^{-1}. The lack of complexity in the low energy region indicates a high degree of molecular symmetry and the pattern in the cyanide stretching region strongly suggests that the geometrical structure of $Mo(CN)_7{}^{4-}$ in the *anhydrous* potassium salt is the same as in aqueous solution.

Infrared spectral data consistent with a pentagonal-bipyramidal structure for $Mo(CN)_7{}^{4-}$ have also been obtained from a partially characterized, hydrated cesium salt, $Cs_4Mo(CN)_7 \cdot xH_2O$.[5] In addition to strong water bands at about 3455 and 1627 cm^{-1}, two cyanide stretching bands are found at 2077 and 2034 cm^{-1}, and a low-energy band is found at 353 cm^{-1} similar to the low-energy band at 358 cm^{-1} in anhydrous $K_4Mo(CN)_7$.

Magnetic Properties. The gram-susceptibility of $K_4Mo(CN)_7 \cdot 2H_2O$ was found to be 2.28×10^{-6} cm^3 g^{-1} at 298°K, corresponding to a magnetic moment of 1.73 BM. Within experimental error, the moment is constant down to 90°K, in essential agreement with the results of a previous study.[6] The magnetic moment of the anhydrous potassium salt was found to be 1.80 BM at 296°K, and a 0.13 *F* aqueous solution exhibited a magnetic moment of 1.6 BM. All of these results indicate a spin-doublet ground state for the d^3 complex and rule against a dimeric or polymeric formulation employing metal-metal bonds or cyano bridging.

---

(5) The cesium salt was prepared by adding water to a 5:1 stoichiometric mixture of solid CsCl and $K_4Mo(CN)_7 \cdot 2H_2O$ until only a small percentage of the solids remained undissolved. The solution was warmed slightly until all solids dissolved and then cooled at 4°. The precipitate, which appeared to be largely CsCl, was separated from the solution, redissolved in H_2O, and crystallized from 30% aqueous ethanol by cooling to 0°. The dark green fine powder which was obtained was washed with 80% ethanol, ethanol, and ether, and dried under vacuum.

(6) J. Lewis, R. S. Nyholm, and P. W. Smith, *J. Chem. Soc.*, 4590 (1961).

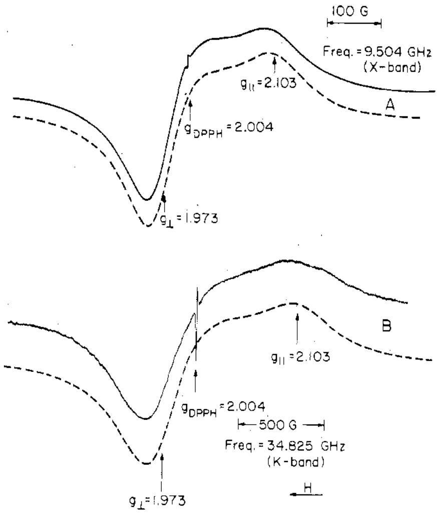

Figure 3. Experimentally observed and computer-simulated esr spectra for the ion $Mo(CN)_7^{4-}$ in an undiluted powder sample of $K_4Mo(CN)_7 \cdot 2H_2O$ (broken curves represent the simulated spectra): (A) X-band spectra (9.50 GHz) at 77°K; (B) K-band spectra (34.80 GHz) at 90°K.

No esr signal was observed at room or liquid nitrogen temperature for aqueous solutions of $K_4Mo(CN)_7 \cdot 2H_2O$ or for the anhydrous potassium salt, $K_4Mo(CN)_7$. Solid $K_4Mo(CN)_7 \cdot 2H_2O$ does give a detectable esr signal in the $g \approx 2$ region, but only below 150°K. The esr spectra, both X band and K band, observed for an undiluted powder sample of $K_4Mo(CN)_7 \cdot 2H_2O$ at liquid nitrogen temperature, are shown together with the computer-simulated spectra in Figure 3. The signal line width was found to decrease substantially on lowering the temperature below 150°K. This line width decrease was accompanied by a concomitant increase in the signal amplitude and the absorption intensity.

The esr spectra shown in Figure 3 are characteristic of a polycrystalline sample of an $S = 1/2$ paramagnetic ion with an axial g tensor. The observed spectra, which are marked with the resonance peak of a DPPH sample, indicate clearly that $g_{\parallel} > 2.00$ and $g_{\perp} < 2.00$ for $K_4Mo(CN)_7 \cdot 2H_2O$. The anisotropy in the g tensor is confirmed by the K-band (34.80 GHz) spectrum in which the separation between the $g_{\parallel}$ and $g_{\perp}$ regions is increased by roughly a factor of 4 over that observed at X band (9.50 GHz). It is unlikely that the esr spectra observed for $Mo(CN)_7^{4-}$ are due to exchange interaction between neighboring Mo(III) species, since no extra resonance attributable to zero-field splitting was observed. In addition, the esr absorption intensity observed here was found to increase with decreasing temperatures, which is characteristic of a paramagnetic system. In contrast, antiferromagnetic exchange would lead to a decrease in absorption intensity on lowering the temperature, whereas temperature-independent intensity should accompany ferromagnetic exchange.

Computer simulation of the first-derivative line shapes employing a method described elsewhere[7] appears to fit the observed spectra. The best fit is obtained using a Lorentzian line shape function with the resonance field $H(\theta)$ calculated from the equation

$$H(\theta) = [(g_{\parallel}^2 \cos^2 \theta + g_{\perp}^2 \sin^2 \theta)\beta^2]^{-1/2} h\nu$$

where each symbol has its conventional meaning. Terms arising from the nuclear hyperfine interaction were not included in the calculations because the hyperfine structure from ^{95}Mo or ^{97}Mo was not observed. The simulated spectra give $g_{\parallel} = 2.103 \pm 0.005$ and $g_{\perp} = 1.973 \pm 0.005$ at both X-band and K-band frequencies.

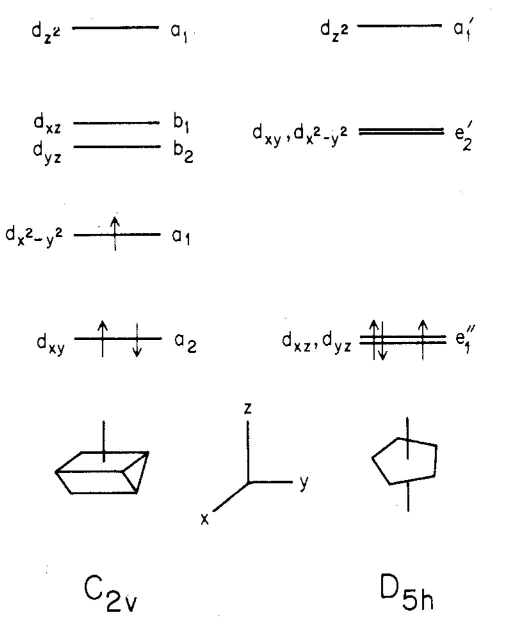

Figure 4. Ligand field energy level diagrams and ground-state electronic configurations for monocapped trigonal-prismatic (C_{2v}) and pentagonal-bipyramidal (D_{5h}) isomers of $Mo(CN)_7^{4-}$.

Ligand field energy level diagrams and ground-state electronic configurations for both pentagonal-bipyramidal and monocapped trigonal-prismatic isomers of $Mo(CN)_7^{4-}$ are shown in Figure 4. The fact that a small distortion from idealized D_{5h} symmetry would be expected for a $^2E_1''(e_1'')^3$ ground state does not alter our principal aqueous solution structural conclusion based on the vibrational spectral data. However, both infrared and Raman spectra, and esr g values, are inconsistent with pentagonal-bipyramidal $^2E_1''(e_1'')^3$ $Mo(CN)_7^{4-}$ in a solid sample of $K_4Mo(CN)_7 \cdot 2H_2O$.[8] In fact, the observed g values require a $^2A_1(a_2)^2(a_1)^1$ ground state and an ordering of low-lying excited states implied by the C_{2v} splitting diagram in Figure 4. The idealized seven-coordinate geometrical structure most likely to lead to the $^2A_1(a_2)^2(a_1)^2$ ground state in question is a monocapped trigonal prism, a structure found recently by Lewis and Lippard[9] for $Mo(CNR)_6I^+$ (R = *tert*-butyl). Taking a value of 204 cm^{-1} for the 4d (Mo) spin-orbit coupling constant (λ) along with reasonable ligand field spectral assignments (*vide infra*), we calculate[10] $g_z = 2.103$, $g_x = 1.983$, and $g_y = 1.984$ for the $^2A_1(a_2)^2(a_1)^1$ ground state of C_{2v} $Mo(CN)_7^{4-}$. The calculated g values are thus in very satisfactory agreement with those experimentally observed ($g_{\parallel} = g_z = 2.103$, $g_{\perp} = g_x \approx g_y = 1.973$).

A monocapped trigonal-prismatic structure for $K_4Mo(CN)_7 \cdot 2H_2O$ is further consistent with the multitude of low-energy infrared bands. Although six infrared bands are predicted to occur in the cyano stretching region for a C_{2v} structure, the axial symmetry indicated by the esr would mean that the upper face of the trigonal prism

---

[7] F.-D. Tsay, H. B. Gray, and J. Danon, *J. Chem. Phys.*, 54, 3760 (1971).

[8] For a $^2E_1''(e_1'')^3$ ground state we would expect to find $g_{\parallel} = g_z \cong 2.0023$.

[9] D. F. Lewis and S. J. Lippard, *Inorg. Chem.*, 11, 621 (1972).

[10] Theoretical expressions for the g values are as follows: $g_z = 2.0023 - 8\lambda/\Delta E(^2A_2 - ^2A_1)$; $g_x = 2.0023 - 2\lambda/\Delta E(^2B_2 - ^2A_1)$; $g_y = 2.0023 - 2\lambda/(\Delta E(^2B_1 - ^2A_1)$.

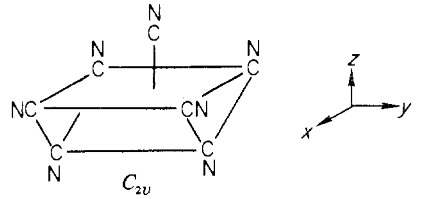

would be nearly square with the *x* and *y* directions nearly equivalent in this plane. Consequently, some of the modes would approach accidental degeneracy. The apparent low-temperature resolution of the cyano stretching region into several closely spaced peaks (Figure 2) is consistent with this interpretation. Finally, we note that a structure in which one or two water molecules coordinate to the open facial positions of the monocapped trigonal prism would be equally consistent with the infrared, Raman, and esr spectral data we have presented for solid $K_4Mo(CN)_7 \cdot 2H_2O$.

Electronic Spectra. The room-temperature electronic absorption spectrum of a rigorously deoxygenated aqueous solution of $K_4Mo(CN)_7 \cdot 2H_2O$, which was prepared in the absence of ≤610-nm light, is presented in Figure 5. Strong bands are located at 216 and 289 nm, and a prominent shoulder is observed at 402 nm. Shoulders at 320, 260, and 245 nm, which are faintly discernible at room temperature, are much better resolved in spectra taken at low temperatures (~90°K) in glasses formed from concentrated LiCl solutions of heptacyanomolybdate(III). Oxidation and photodecomposition products of $Mo(CN)_7^{4-}$ have bands in the region 600–650 nm.[11] Noticeable photodecomposition can occur as the spectrum is being taken, particularly in the more highly concentrated solutions. Such photodecomposition can be largely prevented by having a large excess of cyanide ion in the solution. The spectrum of a 0.015 *F* solution of $Mo(CN)_7^{4-}$ in a 3 *F* KCN solution is essentially identical with that obtained using cyanide-free water as a solvent. In the cyanide-containing solutions, no bands with $\epsilon > 0.5$ are observed in the near-infrared and visible regions at wavelengths greater than 500 nm.

Single crystals of $K_4Mo(CN)_7 \cdot 2H_2O$ were obtained which were thin enough to allow spectral studies from the near-infrared region down to 350 nm at room and liquid N_2 temperature (Figure 6). At room temperature, the only distinct band above 420 nm has a maximum in the 600-nm region. The corrected peak position was found to be 620 nm. When the crystal is cooled to 78°K, the 620-nm band sharpens and shoulders suggesting bands with maxima at 402, 444, and 479 nm are revealed. The ϵ of the 620-nm band was determined to be 15 ± 3.

The electronic spectral results for $K_4Mo(CN)_7 \cdot 2H_2O$ are summarized in Table I. The intensity of the peak at 620 nm (16,100 cm^{-1}) in crystalline $K_4Mo(CN)_7 \cdot 2H_2O$ suggests that it be assigned to a spin-allowed d-d transition in the C_{2v} $Mo(CN)_7^{4-}$ complex. Assuming the C_{2v} ligand field splitting diagram shown in Figure 4, we assign the 16,100-cm^{-1} band to the transition $^2A_1 \rightarrow {}^2A_2$ ($a_2 \rightarrow a_1$). The shoulders at 20,900 and 22,500 cm^{-1} are then attributed to the transitions $^2A_1 \rightarrow {}^2B_2$ ($a_1 \rightarrow b_2$) and $^2A_1 \rightarrow {}^2B_1$ ($a_1 \rightarrow b_1$), respectively.

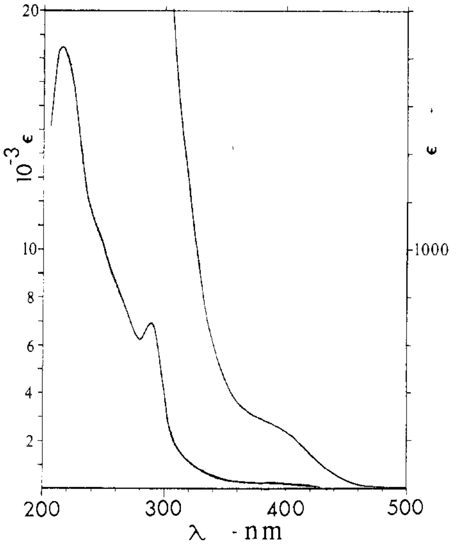

Figure 5. Electronic absorption spectrum of a 0.015 *F* aqueous solution of $K_4Mo(CN)_7 \cdot 2H_2O$.

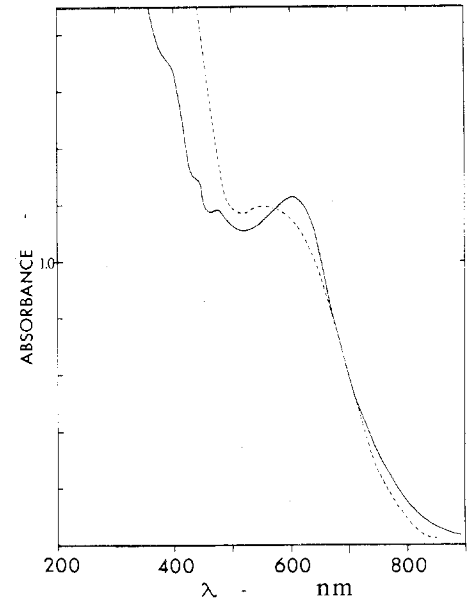

Figure 6. Electronic absorption spectra of a single crystal (~0.065-mm thickness) of $K_4Mo(CN)_7 \cdot 2H_2O$: 26°C, dashed line; 78°K, solid line.

Table I. Electronic Spectral Data for $K_4Mo(CN)_7 \cdot 2H_2O$

Aqueous solution			Solid		
λ, nm	$10^{-3}\bar{\nu}$, cm^{-1}	ϵ	λ, nm	$10^{-3}\bar{\nu}$, cm^{-1}	ϵ
216	46.3	18,400	269	37.2	
245	40.8	sh (liq N_2)	289	34.6	
260	38.5	sh (liq N_2)	323	31.0	
289	34.6	6900	402	24.9	
320	31.2	sh (liq N_2)	444	22.5	sh (liq N_2)
402	24.9	230 sh	479	20.9	sh (liq N_2)
			620	16.1	15 ± 3

Comparison of crystal and aqueous solution spectral data shows that the lowest spin-allowed d-d transition occurs at much higher energy for D_{5h} $Mo(CN)_7^{4-}$ than for the C_{2v} isomer, as expected from simple ligand field considerations (Figure 4). The band at 24,900 cm^{-1} (ϵ ~230) in the solution spectrum may be assigned as the lowest spin-allowed component of the $e_1'' \rightarrow e_2'$ transition.

In both C_{2v} and D_{5h} isomers of $Mo(CN)_7^{4-}$ charge-transfer bands of the type $d \rightarrow \pi^*(CN)$ may be anticipated, in view of the strongly reducing nature of the central Mo(III). The rich ultraviolet spectra of these complexes presumably exhibit both $d \rightarrow \pi^*(CN)$ and higher energy d-d transitions,

---

(11) G. R. Rossman, Ph.D. Thesis, California Institute of Technology, 1971.

but at the present time a detailed assignment of this region is not possible.

Registry No. $K_4Mo(CN)_7\cdot 2H_2O$, 37838-58-7; $K_4Mo(CN)_7$, 37838-59-8; $Cs_4Mo(CN)_7\cdot xH_2O$, 37838-60-1.

Acknowledgments. This research was supported by the Army Research Office–Durham. We thank Professor A. W. Adamson for stimulating our interest in cyanomolybdate chemistry and for several helpful discussions.

Contribution from the Department of Chemistry, Simon Fraser University, Burnaby 2, British Columbia, Canada

Crystal Structure at −100° of Ammonium Oxoperoxo(pyridine-2,6-dicarboxylato)vanadate(V) Hydrate, $NH_4[VO(O_2)(H_2O)(C_5H_3N(COO)_2)]\cdot xH_2O$ ($x \approx 1.3$)

R. E. DREW and F. W. B. EINSTEIN*

Received August 23, 1972

The crystal structure at −100° of the compound $NH_4[VO(O_2)(H_2O)(C_5H_3N(COO)_2)]\cdot xH_2O$ ($x \approx 1.3$) has been determined from three-dimensional X-ray intensity data collected by counter methods on a computer-controlled diffractometer using a Joule-Thomson low-temperature device. The compound crystallizes in the monoclinic space group C_2/c with eight formula units in a cell having lattice constants $a = 11.307$ (2) Å, $b = 25.490$ (5) Å, $c = 8.316$ (2) Å, and $\beta = 96.90$ (1)° (at temperature −100 (2)°). The structure was solved by direct methods and refinement by full-matrix least-squares methods has given a conventional R value of 3.1% for the 1331 observed reflections. The structure is comprised of two crystallographically different ammonium ions (one lying on a twofold axis and the other on a center of symmetry) and a vanadium-based anion. These ions are held together by both electrostatic forces and extensive hydrogen bonding. The vanadium atom environment is a seven-coordinate distorted pentagonal bipyramid, with a vanadyl oxygen and a water molecule at the apices and a peroxy group, the nitrogen from the pyridine ring, and one oxygen atom from each carboxylate group forming an approximate pentagonal plane. The vanadium atom is displaced 0.25 Å from the "plane" toward the vanadyl oxygen atom. Interatomic distances within the anion are 1.870 (2) and 1.872 (2) Å for the $V-O_{peroxo}$ bonds, 1.579 (2) Å for the V=O bond, 2.053 (2) and 2.064 (2) Å for the $V-O_{carboxylate}$ distances, 2.211 (2) Å for the $V-O_{water}$ distance, 2.088 (2) Å for the V–N distance, and 1.441 (2) Å for the $O-O_{peroxo}$ bond.

Introduction

Structural data on transition metal-peroxo compounds have recently been extended to include the peroxovanadates with the elucidation of the structures of $NH_4[VO(O_2)_2(NH_3)]$,[1] $(NH_4)_4[O(VO(O_2)_2)_2]$,[2] and $(NH_4)_3[V(O_2)_4]$.[2,3] The mononuclear oxodiperoxoamminevanadate(V) anion was shown[1] to have a distorted pentagonal-pyramidal geometry, analogous to the oxodiperoxopyridinechromium(VI) complex,[4] $CrO(O_2)_2(C_5H_5N)$, while the dinuclear $[O(VO(O_2)_2)_2]^{4-}$ anion was demonstrated[2] to have distorted pentagonal-bipyramidal coordination geometry around each vanadium atom. The tetraperoxovanadate(V) anion[2,3] has a quasidodecahedral structure as does the tetraperoxoniobate(V) compound,[5] $KMg[Nb(O_2)_4]\cdot 7H_2O$, and the tetraperoxochromium(V) compound,[6] $K_3[Cr(O_2)_4]$. It has been proposed[7] that the triperoxovanadates could have eight-coordination of the metal similar to that observed in the peroxoniobate(V) compounds $K[Nb(O_2)_3(C_{12}H_8N_2)]\cdot 3H_2O$,[8] $K[Nb(O_2)_3(C_{12}H_8N_2)]\cdot 3H_2O\cdot H_2O_2$,[8] and $(NH_4)_3[Nb(O_2)_2(C_2O_4)_2]\cdot H_2O$.[9] To continue the structural study of peroxovanadates, the crystal structure of the monoperoxy complex $NH_4[VO(O_2)(H_2O)(C_5H_3N(COO)_2)]\cdot xH_2O$ ($x \approx 1.3$) has been determined and work on the compounds $K_3[VO(O_2)(C_2O_4)_2]$ and $K_3[VO(O_2)_2(C_2O_4)]$ is in progress.

Experimental Section

The preparation of ammonium oxoperoxo(pyridine-2,6-dicarboxylato)vanadate(V) hydrate, $NH_4[VO(O_2)(H_2O)(C_5H_3N(COO)_2)]\cdot xH_2O$ ($x \approx 1.3$), as was first reported by Hartkamp[10,11] was used. This method involved the reaction of ammonium vanadate, pyridine-2,6-dicarboxylic acid, and hydrogen peroxide in the ratio 1:1:1 to give dark red crystals. A crystal fragment of maximum dimensions 0.46 × 0.25 × 0.34 mm in the directions a, b, and c, respectively, was selected and mounted with the longest dimension approximately parallel to the rotation axis. This single crystal yielded the complete diffraction data (obtained over a period of *ca.* 2 weeks); no decomposition was observed.

Weissenberg photographs of the $0kl$–$3kl$ layers and precession photographs of the $hk0$–$hk1$ and $h0l$–$h2l$ layers using Cu Kα radiation showed absences for hkl, $h + k = 2n + 1$; $h0l$, $l = 2n + 1$ ($h = 2n + 1$). This, combined with Laue symmetry ($2/m$), indicated the space group as either Cc or C_2/c. (Our work indicates that the centrosymmetric space group C_2/c provides a satisfactory model.)

Crystal Data

Data are as follows for $NH_4[VO(O_2)(H_2O)(C_5H_3N(COO)_2)]\cdot xH_2O$ ($x = 1.311$ (8)): mol wt 323.6, monoclinic, $a = 11.307$ (2) Å, $b = 25.490$ (5) Å, $c = 8.316$ (2) Å, $\beta = 96.90$ (1)°, $V = 2379.42$ (1) Å^3 (at −100 (2)°), $d_m = 1.74$ (5) g/cm^3 (at 22°), $Z = 8$, $d_c = 1.79$ g/cm^3 (at 22°), $d_c = 1.83$ g/cm^3 (at −100°), $F(000) = 1320$, μ(Mo Kα) 10.0 cm^{-1}, λ(Cu Kα) 1.5418 Å, λ(Mo Kα_1) 0.70926 Å.

It was decided that the data be collected at low temperature because of the rapid falloff in the average reflection's intensity with increasing 2θ. To measure the reflection intensities for the unique set of data at −100°, an Air Products and Chemicals

---

[1] R. E. Drew and F. W. B. Einstein, *Inorg. Chem.*, 11, 1079 (1972).

[2] I.-B. Svensson and R. Stomberg, *Acta Chem. Scand.*, 25, 898 (1971).

[3] I.-B. Svensson, *Acta Chem. Scand.*, to be submitted for publication.

[4] R. Stomberg, *Ark. Kemi*, 22, 29 (1964).

[5] G. Mathern and R. Weiss, *Acta Crystallogr., Sect. B*, 27, 1598 (1971).

[6] R. Stomberg, *Acta Chem. Scand.*, 17, 1563 (1963).

[7] J. Sala-Pala and J. E. Guerchais, *J. Chem. Soc. A*, 1132 (1971).

[8] G. Mathern and R. Weiss, *Acta Crystallogr., Sect. B*, 27, 1582 (1971).

[9] G. Mathern and R. Weiss, *Acta Crystallogr., Sect. B*, 27, 1572 (1971).

[10] H. Hartkamp, *Angew. Chem.*, 71, 553 (1959).

[11] H. Hartkamp, *Z. Anal. Chem.*, 171, 262 (1959).